

Solid solution strengthening of Ni₃Al by B and Hf additions

F. Heredia, D. Pope

► **To cite this version:**

F. Heredia, D. Pope. Solid solution strengthening of Ni₃Al by B and Hf additions. Journal de Physique III, EDP Sciences, 1991, 1 (6), pp.1055-1064. <10.1051/jp3:1991171>. <jpa-00248625>

HAL Id: jpa-00248625

<https://hal.archives-ouvertes.fr/jpa-00248625>

Submitted on 1 Jan 1991

HAL is a multi-disciplinary open access archive for the deposit and dissemination of scientific research documents, whether they are published or not. The documents may come from teaching and research institutions in France or abroad, or from public or private research centers.

L'archive ouverte pluridisciplinaire **HAL**, est destinée au dépôt et à la diffusion de documents scientifiques de niveau recherche, publiés ou non, émanant des établissements d'enseignement et de recherche français ou étrangers, des laboratoires publics ou privés.

Classification
Physics Abstracts
81.40C — 81.40L

Solid solution strengthening of Ni₃Al by B and Hf additions

F. E. Heredia and D. P. Pope

Department of Materials Science and Engineering, University of Pennsylvania, 3231 Walnut Street, Philadelphia, PA, 19104-6276, U.S.A.

(Received June 19, 1990, accepted September 20, 1990)

Résumé. — La limite élastique de Ni₃Al peut être considérablement augmentée par l'addition de différents éléments d'alliage ternaires. Certains d'entre eux provoquent un renforcement plus ou moins uniforme dans tout un domaine de température (B, par exemple) tandis que d'autres, tels Hf, sont la cause d'un durcissement à basse température suivi d'une augmentation plus rapide de la limite élastique avec la température. En d'autres termes, l'anomalie de limite élastique est accentuée par l'addition de Hf, mais pas de B. Le renforcement de Ni₃Al par ces deux éléments est interprété en termes d'une combinaison de durcissement par solution solide, et de durcissement par glissement dévié. Nous montrons que Hf semble renforcer Ni₃Al par une combinaison de durcissement par solution solide et par augmentation du taux de déviation (ce qui correspond à une diminution de l'énergie d'activation du glissement dévié), tandis que B semble seulement durcir par effet de solution solide.

Abstract. — The yield stress of Ni₃Al can be greatly increased by the addition of various ternary alloying elements. Some of these cause a more or less uniform strengthening over a range of temperatures, e.g. B, while others like Hf cause strengthening at low temperatures and a more rapid increase in the flow stress with temperature, i.e. the flow stress anomaly is increased by Hf, but not by B. The strengthening of Ni₃Al by these two elements is interpreted in terms of a combination of solid solution hardening and cross-slip hardening. It is shown that Hf appears to strengthen Ni₃Al by a combination of solid solution hardening and increased cross-slip (leading to a decreased activation energy for cross-slip), while B appears to only strengthen by solid solution hardening.

1. Introduction.

Ni₃Al is an extremely important material both from a technological and scientific point of view. From a technological point of view it is important because Ni₃Al — based precipitates comprise the largest volume fraction of modern Ni-base superalloys. Also, since the yield stress-temperature behavior of Ni₃Al shows a strong anomaly (yield stress increases as a function of temperature up to some maximum at a temperature around 800 K then decreases again) there is great scientific interest in the causes of this anomaly. This anomalous behavior is observed in many alloys with the crystal structure of Ni₃Al, the so-called L1₂ structure

which has A atoms on the face centers and B atoms on the corners of an fcc unit cell forming an A_3B compound. Among these alloys are Ni_3Ga , Ni_3Ge and Ni_3Si , in addition to Ni_3Al . Ni_3Al has great technological utility because its properties can be markedly changed by changing stoichiometry or by alloying with ternary elements. Ni_3Al has a stable compositional range of several atomic percent and has a high solubility for many additional elements [1].

The flow behavior of Ni_3Al is very complex when contrasted with that of simple materials such as copper, but it must be emphasized that there are very few such simple materials. In this context we define a simple material as one in which the onset of plastic flow at low temperatures is controlled by the resolved shear stress (RSS) on the slip plane in the slip direction of the moving dislocations, i.e. Schmid's Law applies. In such materials dislocation motion commences at a critical value of the RSS, changes in uniaxial flow strength are reflected by changes in the Schmid factor, and *only glide* components of the stress tensor are important [2], e.g. hydrostatic pressure has no effect, and the sense of the RSS also has no effect. The number of materials in this category of simple materials is extremely limited, consisting of fcc metals and hcp metals which deform by basal slip. In such materials dislocations glide on the close packed plane, the Burgers vectors are equal to the nearest neighbor distance, the flow stress is not strongly temperature-dependent at low temperatures, and the flow stress is the same in tension and in compression. However, when one considers the plastic flow of even mildly complicated materials such as bcc metals, not to mention intermetallic compounds, the picture rapidly becomes more complex. In these materials dislocations do not always glide on the close packed planes ; the magnitude of the Burgers vector can be extremely complicated ; and several non-glide components of the stress tensor can simultaneously become important. These factors commonly lead to a breakdown of Schmid's Law and a strong temperature dependence of the yield strength, especially at low temperatures.

We take the point of view of Vitek [2] that the differences between simple materials (which form the great majority of crystalline materials) and complex ones can be understood to a large part by differences in dislocation core structures. In simple materials the dislocations with the lowest energy also happen to be the ones which have the highest mobility. That is, dislocations on the (111) planes of fcc and (0001) planes of hcp with Burgers vectors equal to the nearest neighbor distances can always dissociate into a highly mobile planar configuration consisting of two Shockley partial dislocations separated by stacking fault. This fault is always stable, based on symmetry considerations. When the Shockley partials are widely separated in materials with low stacking fault energy, to the extent that the cores do not overlap, they can be clearly identified as individual dislocations, but when the fault energy is high, the cores do overlap. However in either case dislocations are planar, i.e. they are spread on the close packed plane, and are always highly mobile. In more complex materials the dissociations are more complex, commonly leading to non-planar cores, as is the case of screw dislocations in bcc metals. In such a case, the applied stress tensor must not only force the core into a planar configuration, a process involving both stress and thermal activation, and the stress forcing the core into a planar form is not necessarily the one causing glide. This results in a breakdown of Schmid's Law.

The difficulty in understanding the rate-controlling processes in these non-simple materials comes from the necessity of somehow first understanding how the dislocation dissociates and then deciding which components of the stress tensor are important. From now on we will concentrate on $L1_2$ materials. The precise mechanism by which the flow anomaly occurs in these materials is not without controversy, as will be discussed later in this paper. However, there is general agreement, based on the competing theories put forward, that nonplanar dislocation core configurations are the fundamental causes of the anomalies observed.

2. Flow behavior of L₁₂ materials.

The flow behavior of L₁₂ materials can either be anomalous, like Ni₃Al, or normal, like Pt₃Al, as shown in figures 1a and 1b, respectively. In the balance of this paper we concentrate on the anomalous behavior since, to the best of our knowledge, there have been no studies of solid solution strengthening in L₁₂ materials showing the normal behavior. The important features of the anomalous flow behavior in Ni₃Al are the following (see Refs. [3] and [4] for more details) :

- 1) The flow stress of a given polycrystalline material tested at a given strain rate is a function only of the test temperature over the entire flow stress curve [5], i.e. a single sample can be tested at many different temperatures and show flow stresses lying on the curve in figure 1a, independent of the order of testing (with small corrections for work hardening).
- 2) The strain rate sensitivity in the anomalous portion of the flow stress temperature curve is small but positive [4]. This indicates that diffusion-controlled processes are not important in this temperature regime.
- 3) In the anomalous portion of the flow stress-temperature curve slip occurs by the motion of $[\bar{1}01]$ (111) dislocations for samples oriented in the standard [001]-[011]- $[\bar{1}11]$ unit triangle [6, 7].
- 4) Deformation at temperatures above T_p of non-cube oriented samples occurs by slip on the $[\bar{1}10]$ (001) cube system [7, 8].
- 5) Cube slip can occur at low temperatures, as low as room temperature, if the RSS is sufficiently high, i.e. for near $-\bar{1}11$ oriented samples [7].
- 6) The CRSS for slip on the system in the anomalous region depends on the RSS on the $[\bar{1}01]$ (010) system [9].
- 7) The CRSS for $[\bar{1}01]$ (111) slip is different in tensile and compressive tests and the difference varies in a smooth way across the unit triangle [10-13].

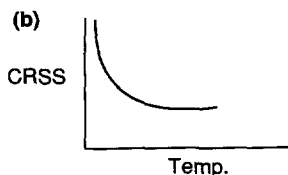
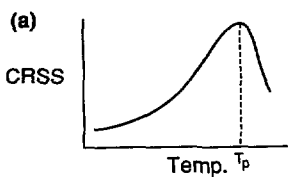


Fig. 1.

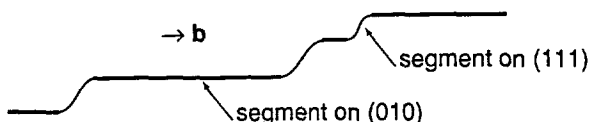


Fig. 2.

Fig. 1. — Flow behavior seen in L₁₂. (a) anomalous, (b) normal.

Fig. 2. — Configuration of dislocations usually seen in the anomalous temperature regime in Ni₃Al. The segments on (010) planes are pure screw while those on (111) planes are mixed.

- 8) The flow stress in the anomalous region depends strongly on the offset plastic strain used. For small offset strains, 10^{-5} or less, the flow stress is almost temperature-independent, whereas for offset strains of 10^{-3} the anomaly is clearly visible [6, 14].
- 9) The dominant dislocation structure seen after deformation in the anomalous region is long, straight screws having the $[\bar{1}01]$ Burgers vector [6, 14, 15].
- 10) Above the peak temperature the CRSS shows a large, positive strain rate dependence for both $[\bar{1}10]$ (001) [12, 16] and $[\bar{1}01]$ (111) slip [16].
- 11) The long, straight $[\bar{1}01]$ screws dislocations seen in samples deformed below T_p tend to have the configuration shown in figure 2, i.e. the screw portions are dissociated on the (010) plane and the non-screws are dissociated on (111) [17-20].

3. Cross-slip model.

This model is based on the original suggestion of Flinn [5] that the APB energy on (111) planes of Ni_3Al should be much higher than on (010) planes. This is the basis for the Kear-Wiltsdorf cross-slip model [21-22] (Fig. 3) in which it is suggested that screw dislocations can lower their energy by cross-slipping from (111) planes, where they are mobile, to (010) planes where they are sessile. These two ideas were incorporated into the theory of Takeuchi and Kuramoto [23] to explain the anomalous flow behavior of Ni_3Ga . In this model, it is assumed that localized segments of screw dislocations cross-slip from the (111) plane to the (010) plane, then serve as pinning points which retard subsequent motion on the (111) plane. The driving force for this cross-slip was assumed to be both the anisotropy of the APB energy and the RSS on the $[\bar{1}01]$ (010) system, i.e. the RSS driving cube cross-slip. This model was later modified by Lall *et al.* [7] and Paidar *et al.* [24] to include the effects of the tension/compression flow asymmetry for $[\bar{1}01]$ (111) slip. One of the great success of the cross-slip model was the correct prediction of the sense and orientation dependence of this tension/compression [T/C] asymmetry by Paidar *et al.* [24]. The trends with orientation predicted and later confirmed by Umakoshi *et al.* [11] are shown in figure 4. The energetics of the Paidar *et al.* model were later modified by Yoo [25-27] to include the effects of anisotropic elasticity which result in a torque that assists in driving the leading $1/2 [\bar{1}01]$ superpartial onto the (010) plane.

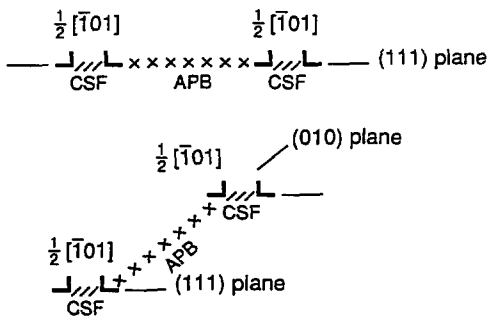


Fig. 3.

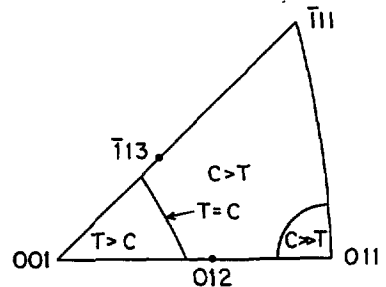


Fig. 4.

Fig. 3. — The Kear-Wiltsdorf cross-slip mechanism.

Fig. 4. — Predictions of the model of Paidar *et al.*

The prediction of the model with all the above additions is :

$$\Delta\tau = B \exp(-H/kT) \tag{1}$$

$$H = W + b \left\{ \frac{\mu b^2}{8\pi} - \left[\frac{\mu b^3}{8\pi} F \right]^{1/2} \right\} \tag{2}$$

$$F = \gamma_1(1 + f_1 \sqrt{2})/\sqrt{3} - \gamma_0 + \tau_{cb} b \tag{3}$$

$$f_1 = \sqrt{2}(A - 1)/(A + 2) \tag{4}$$

$$A = 2 C_{44}/(C_{11} - C_{12}), \tag{5}$$

where $\Delta\tau$ is the increase in the CRSS for $[\bar{1}01]$ (111) slip over the low temperature value ; B is a constant ; k is Boltzmann's constant ; T is temperature ; W is a factor which includes the T/C asymmetry ; μ is the shear modulus ; b is $1/2 [\bar{1}01]$; τ_{cb} is the RSS on $[\bar{1}01]$ (010) ; γ_1 and γ_0 are APB energies on (111) and (010) planes, respectively ; C_{44} , C_{11} and C_{12} are elastic constants ; and A is the anisotropy ratio of Zener. The predictions of this model have agreed remarkably well with the experimental observations in the temperature region below T_p . It is therefore a reasonable starting point to explain the solid solution strengthening of Ni₃Al and will be used here. If F is > 0 for all orientations of the stress axis, including [001] for which $\tau_{cb} = 0$, then the flow stress always increases with temperature. Recent observations of APB anisotropy combined with the elastic anisotropy do indicate that $\gamma_1(1 + f_1 \sqrt{2})/\sqrt{3} - \gamma_0$ is, indeed, greater than zero even though it appears that $\gamma_1/\sqrt{3} - \gamma_0$ is negative [26, 28].

However there is one important recent set of observations on Ni₃Al which cannot be explained by the model : the *in situ* TEM observations of Caillard *et al.* [30] :

- 1) Deformation is carried by long $1/2 [\bar{1}01]$ screw dislocations on (111) planes but *bowing was not observed*.
- 2) Motion of screw dislocations is jerky and the jerks correspond to changes in superpartial spacing. The changes are consistent with changes in the plane of the $1/2 [\bar{1}01]$ dislocation cores from (111) to $(1\bar{1}1)$ and back again.
- 3) Dislocations were seen to move from (111) to (010) planes *and back again*.

These observations are discussed in greater detail by Couret and Caillard [31] in this volume, so they will not be further discussed here. Suffice is to say that there is no known way to explain these observations within the confines of the cross-slip model. Caillard *et al.* [30] have proposed an entirely different model that is in accord with their observations in Ni₃Al, and

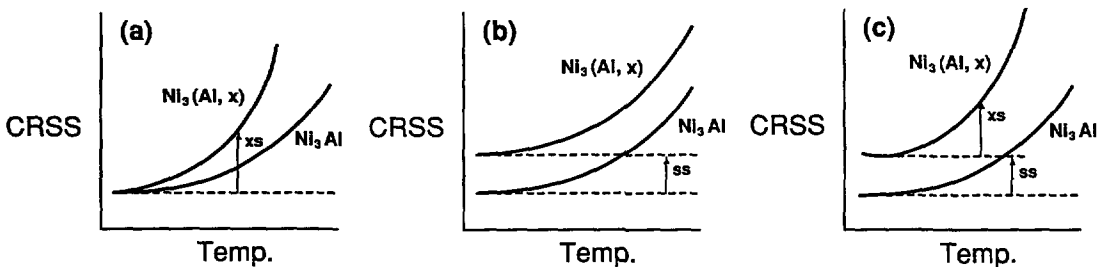


Fig. 5. — Expected changes in the CRSS-temperature curve of Ni₃Al when element X is added to make Ni₃(Al, X).

their observations in Be [32], but the new model does not explain many other observations in section 2 of this paper. (Ref. [4] deals with problems of the various competing models).

Returning now to the cross-slip model, the various kinds of behavior to be expected from the addition of solutes are shown in figure 5. For example, if a solute simply reduces F in equation (3) then the activation energy for cross-slip is reduced, the rate of cross-slip is increased, and the behavior shown in figure 5a is expected. If the solute distorts the lattice, thereby resulting in solid solution strengthening but no change in F , then the behavior in 5b is expected. Finally if solid solution strengthening and increased cross-slip result, then the behavior in 5c is expected. Many different orientations and compositions were tested as part of this study [33], but only the Hf and B containing samples for the $[T = C]$ orientations are reported on here for the sake of brevity.

4. Experimental procedures.

Single crystalline samples were prepared and tested in the manner described by Ezz *et al.* [10] and Heredia [33]. The compositions of the samples are listed in table I. Note that the samples containing 1 % Hf also contain 0.2 % B. (All compositions are given in at%). Briefly stated the experimental procedures are as follows: Single crystalline bars of off-stoichiometric Ni_3Al , grown by the Bridgman technique, containing different additions of Hf and B were obtained from PCC Airfoils Inc., Cleveland, Ohio. The alloys used in this study are off-stoichiometric due to the difficulty of growing stoichiometric crystals and were chosen to be in the Ni-rich side because results reported in the literature show that a rather significant hardening occurs for Al-rich deviated material, but only a small amount of hardening is found for the Ni-rich material. Tensile and compressive tests were performed in an Instron Testing Machine at a nominal strain rate of $1.3 \times 10^{-3} s^{-1}$ at temperatures from 77 to 1 250 K. Tests from room temperature to 1 250 K were carried out in air with the tension/compression system enclosed in a furnace. The CRSS is calculated from the 0.2 % plastic offset axial yield stress.

Table I. — *Chemical composition of the $Ni_3Al + X$ Single Crystals.*

MATERIAL	COMPOSITION (at%)		
	at% Ni	at% Al	at% X
Binary	76.6	23.4	none
1 Hf	75.80	23.00	1.0 Hf + 0.2 B
3.3 Hf	74.80	21.80	3.28 Hf
0.2 B	77.15	22.63	0.195 B
0.7 B	76.77	22.56	0.67 B
1 B	76.52	22.50	0.98 B

5. Experimental results.

The CRSS for $[\bar{1}01] (111)$ slip of the Ni₃(Al, Hf) samples is given as a function of temperature in figure 6a. Note that the rate of increase of the CRSS in the anomalous region increases with Hf additions — that is, the activation energy decreases. (The apparently high CRSS at low temperatures of the 1 % Hf material is probably the result of the 0.2 % B in these samples — the result of obtaining these samples from an alternate supplier. The dotted line at low temperatures in the curve was obtained by subtracting the effects of the 0.2 B. This subtraction was performed by plotting the CRSS vs. Hf content for the binary and for all Hf — containing samples, one plot for each test temperature. Assuming that the CRSS is linear with Hf content, as was observed for Ta and Zr [33], the effect of the B was obtained from the deviation of the 1 % Hf + 0.2 B point from that straight line.) The behavior of the boron — containing samples is shown in figure 6b. Note that B causes relatively large strength increases at low temperatures, but relatively smaller increases at high temperatures. Also note that 0.2 B has almost no effect at high temperatures.

The activation energy for cross-slip is obtained by plotting in $\Delta\tau$ as in figure 7. The resulting activation energies are then plotted as a function of composition in figure 8. It is seen that the

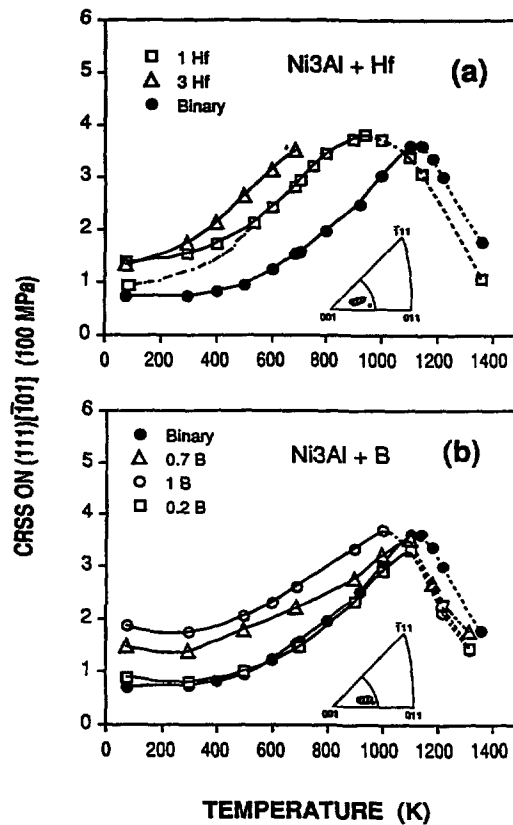


Fig. 6. — The CRSS on $[\bar{1}01] (111)$ as a function of temperature for (a) Ni₃Al + Hf and (b) Ni₃Al + B, in the $[T = C]$ orientation. Dotted lines are shown in the region where slip actually occurs on the $[\bar{1}10] (001)$ system.

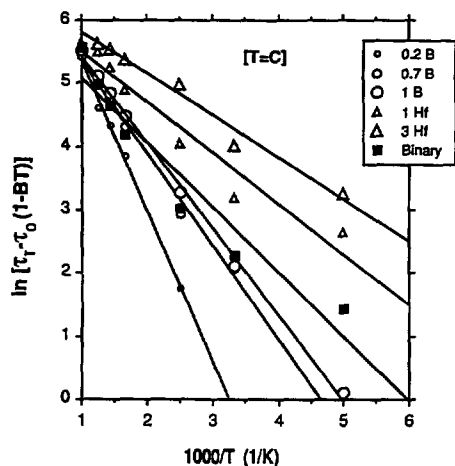


Fig. 7.

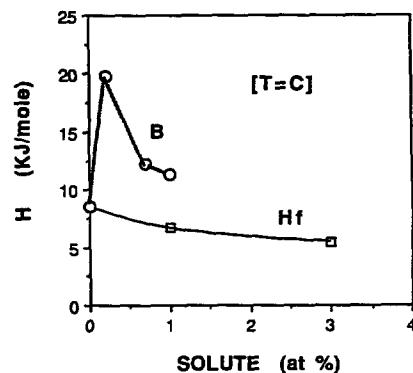


Fig. 8.

Fig. 7. — Arrhenius plots of $\ln \Delta \tau$ vs. $1/T$ for the $[T = C]$ orientations for purposes of extracting an activation energy, H .

Fig. 8. — The activation energy, H , as a function of solute concentration.

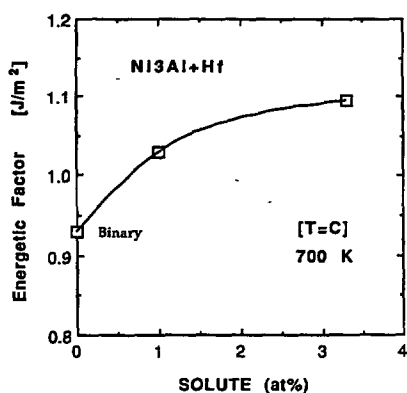


Fig. 9.

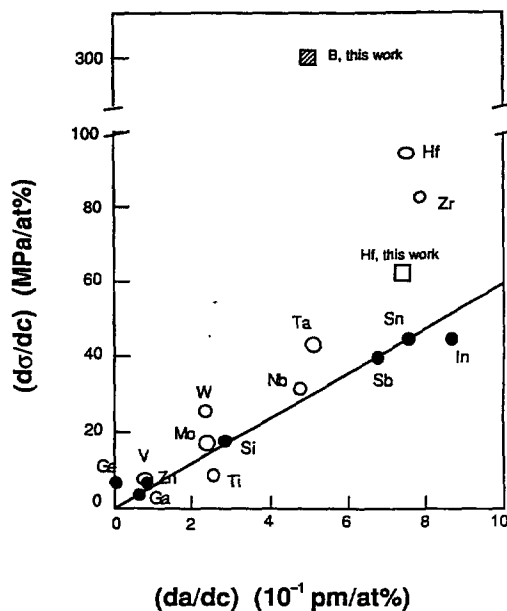


Fig. 10.

Fig. 9. — The energetic factor as a function of Hf content.

Fig. 10. — Comparison of the rate of solid solution strengthening of Ni_3Al single crystals at low temperature by Hf and B (this study) with the data of Mishima *et al.*

addition of Hf reduces H, but B seems to increase H. The effect of B is probably not to actually increase H, but rather it causes solid solution strengthening at low temperatures that disappears, due to thermal activation, as the temperature increases. This results in an *apparent* increase in H.

Returning now to equation (1) we extract a factor we call the energetic factor, which is actually $\gamma_1(1 + f_1 \sqrt{2})/\sqrt{3} - \gamma_0$ in equation (3), from the data for the $[T = C]$ orientations, as shown in figure 9 for the Hf-containing material. Note that the energetic factor does increase with increasing Hf concentration, indicating that the energy gained by (010) to (111) cross-slip increases with increasing Hf. (A similar plot is not included for B in figure 9 since it would show a decrease in the energetic factor, but we believe that is only an *apparent* effect, as discussed above).

Finally, we show in figure 10 a plot from Mishima *et al.* [34] in which the increase in strength at low temperatures is correlated with the lattice misfit parameter. The data points for Hf and B from this study are included for comparison. Unfortunately there are no data available on the misfit parameter for B in Ni₃Al, so the correlation cannot be made.

6. Discussion.

The strengthening of Ni₃Al by B and Hf in the temperature regime of octahedral slip can be adequately understood in terms of a combination of ordinary solid solution strengthening and cross-slip. Hf produces a substantial lattice strain in Ni₃Al which results in a large strength increase at low temperatures. B also causes a large strength increase at low temperatures, much larger than for any of the substitutional solutes, as would be expected for an interstitial. The lattice parameter data for B are from Baker *et al.* [35].

The reasons for the decrease in the activation energy for cross-slip due to Hf additions are less easy to explain. The arguments of Wee *et al.* [36, 37] are most commonly cited. They suggest that alloying elements making Ni₃Al unstable relative to DO₂₂ or DO₁₉ should result in an increase in the rate of cross-slip since the DO₂₂ and DO₁₉ structures are related to L₁₂ by periodic faults on (010) and (111) planes, respectively, which cause no nearest neighbor violations. The argument is stronger for the DO₂₂ case, since the (010) fault in this case is the (010) APB. When the DO₂₂ structure becomes stable relative to L₁₂ this fault must have a zero (or negative) energy. In the case of DO₁₉ the situation is less clear, since DO₁₉ and L₁₂ are related by periodic superlattice intrinsic stacking faults on (111) planes of the L₁₂. In this case the (010) APB energy could also be reduced, but at the same time, the (111) APB is also expected to drop, leading to no decrease, or perhaps a net increase, in the driving force for (111) to (010) cross-slip (see Refs. [3] and [19] for more discussion of this point). The structure of one form of Ni₃Hf is DO₁₉ so the suggestion of Wee *et al.* [36, 37] applies, but with the above-stated caveat.

Finally, it should be stated that in a recent study by Dimiduk [19], only very small changes in APB energies on (111) and (010) planes were seen using HREM for both Sn and V additions, and furthermore some of the changes of APB energies actually tend to retard the cross-slip process, even though strengthening was observed. These measurements were made by observing the width of splitting of 1/2 $[\bar{1}01]$ dislocations on the (111) and (010) planes, respectively. Assuming that the rate of cross-slip is increased by alloying additions, the results of Dimiduk and those reported here can only be reconciled by assuming that solutes increase the elastic anisotropy and thereby increase the torque factor, f_1 in equation (3), or that the APB widths observed in the TEM are different from those occurring during deformation. That is, there may be sufficient time for atomic rearrangement to occur, thereby changing fault energies on the time scale of TEM experiments, but such rearrangements do not occur

during deformation processes. This controversy cannot be resolved at this time based on the data available to us.

Acknowledgements.

This research was supported by the office of Naval Research under Grant no. N00014-87-K-0792. Experimental facilities were provided by the LRSM of the University of Pennsylvania supported by the National Science Foundation under grant no. DMR-88-22858.

References

- [1] OCHIAI S., OYA Y. and SUZUKI T., *Acta Met.* **32** (1984) 289.
- [2] VITEK V., In «Dislocations and Properties of Real Crystals» N. H. Loreto, Ed. (Institute of Metals, London) 1985, pp. 30-50.
- [3] POPE D. P. and EZZ S. S., *Int. Met. Rev.* **29** (1984) 136-167.
- [4] POPE D. P., «High Temperature Aluminides and Intermetallics» (S. H. Whang, Ed.), TMS-AIME, Warrendale, PA., to appear 1990.
- [5] FLINN P. A., *Trans. AIME* **218** (1960) 145.
- [6] THORNTON P. H., DAVIES R. G. and JOHNSTON T. L., *Metall. Trans.* **1** (1970) 207.
- [7] LALL C., CHIN S. and POPE D. P., *Metall. Trans.* **10A** (1979) 1323.
- [8] STATON-BEVAN A. E. and RAWLINGS R. D., *Phys. Status Solidi* (a) **29** (1975) 613.
- [9] KURAMOTO E. and POPE D. P., *Acta Met.* **26** (1978) 207.
- [10] EZZ S. S., POPE D. P. and PAIDAR V., *Acta Metall.* **30** (1982) 921.
- [11] UMAKOSHI Y., POPE D. P. and VITEK V., *Acta Metall.* **32** (1984) 449-56.
- [12] EZZ S. S., POPE D. P. and VITEK V., *Acta Metall.* **35** (1987) 1879-1885.
- [13] BONDA N. R., POPE D. P. and LAIRD C., *Acta Metall.* **35** (1987) 2371-2383.
- [14] MULFORD R. A. and POPE D. P., *Acta Met.* **21** (1973) 1375.
- [15] KEAR B. H. and HORNBECKER M. F., *Trans. ASM* **59** (1966) 155.
- [16] MIURA S., MISHIMA Y. and SUZUKI Z., *Z. Metallkde* **80** (1989) 157.
- [17] VEYSSIERE P., In «High Temperature Ordered Intermetallic Alloys III», pp. 175-188 (Materials Research Society, Pittsburgh, PA 1989).
- [18] SUN Y. Q. and HAZZLEDINE P. M., *Philos. Mag. A* **58** (1988) 603.
- [19] DIMIDUK D. M., Ph. D. Dissertation (Carnegie-Mellon University) 1989.
- [20] MILLS M. J., BALUC N. and KARNTHALER H. P., In «High Temperature Ordered Intermetallic Alloys III» (Materials Research Society, Pittsburgh, PA) 1989, pp. 203-215.
- [21] KEAR B. H. and WILSDORF H. G. F., *Trans. AIME* **233** (1962) 714.
- [22] KEAR B. H., *Acta Metall.* **12** (1964) 555.
- [23] TAKEUCHI S. and KURAMOTO E., *Acta Metall.* **21** (1973) 415.
- [24] PAIDAR V., POPE D. P. and VITEK V., *Acta Metall.* **32** (1984) 435.
- [25] YOO M. H., *Acta Metall.* **20** (1986) 915.
- [26] YOO M. H., In «High Temperature Ordered Intermetallic Alloys II, Stoloff N. S., Koch C. C., Liu C. T. and Izumi O. Eds. (Materials Research Society, Pittsburgh, PA) 1987, p. 207.
- [27] YOO M. H., *Acta Metall.* **35** (1987) 1559.
- [28] TAUNT R. J. and RALPH B., *Philos. Mag.* **30** (1974) 1379.
- [29] DOUIN J., VEYSSIERE P. and BEAUCHAMP P., *Philos. Mag.* **54** (1986) 375.
- [30] CAILLARD D., CLEMENT N., COURET A., LOURS P. and COUJOU A., *Philos. Mag. Lett.* **58** (1988) 263.
- [31] COURET A. and CAILLARD D., in this volume.
- [32] COURET A. and CAILLARD D., *Philos. Mag. A.* **59** (1989) 783.
- [33] HEREDIA F. E., Ph. D. Dissertation (University of Pennsylvania) 1990.
- [34] MISHIMA Y., OCHIAI S., YODOGAWA M. and SUZUKI T., *Trans. Japan. Instit. Metals* **27** (1986) 41.
- [35] BAKER I., HUANG B. and SCHULSON E. M., *Acta Metall.* **36** (1988) 493.
- [36] WEE D. M. and SUZUKI T., *Trans. Japan. Inst. Met.* **20** (1979) 634.
- [37] WEE D. M., NOGUCHI O., OYA Y. and SUZUKI T., *Trans. Japan. Inst. Met.* **21** (1980) 237.